Journal of Controlled Release 199 (2015) 106–113

Contents lists available at ScienceDirect

Journal of Controlled Release

journal homepage: www.elsevier.com/locate/jconrel

Polyethylene glycol (PEG)-dendron phospholipids as innovative constructs for the preparation of super stealth liposomes for anticancer therapy

Gianfranco Pasut [a,1], Donatella Paolino [b,c,1], Christian Celia [d,e], Anna Mero [a], Adrian Steve Joseph [a], Joy Wolfram [d], Donato Cosco [b,c], Oddone Schiavon [a], Haifa Shen [d,f], Massimo Fresta [b,c,*]

[a] Department of Pharmaceutical and Pharmacological Sciences, University of Padua, Padua 35131, Italy
[b] Department of Health Science, University "Magna Græcia" of Catanzaro, Catanzaro 88100, Italy
[c] Interregional Research Center for Food Safety & Health, University of Catanzaro "Magna Græcia", Catanzaro 88100, Italy
[d] Department of Nanomedicine, Houston Methodist Research Institute, Houston, TX 77030, USA
[e] Department of Pharmacy, University "G. D'Annunzio" of Chieti-Pescara, Chieti 66013, Italy
[f] Department of Cell and Developmental Biology, Weill Cornell Medical College, New York, NY 10065, USA

ARTICLE INFO

Article history:
Received 19 August 2014
Accepted 8 December 2014
Available online 9 December 2014

Keywords:
Liposome
Pegylation
Polyethylene glycol
Cancer therapy
Phospholipid

ABSTRACT

Pegylation of nanoparticles has been widely implemented in the field of drug delivery to prevent macrophage clearance and increase drug accumulation at a target site. However, the shielding effect of polyethylene glycol (PEG) is usually incomplete and transient, due to loss of nanoparticle integrity upon systemic injection. Here, we have synthesized unique PEG-dendron-phospholipid constructs that form super stealth liposomes (SSLs). A β-glutamic acid dendron anchor was used to attach a PEG chain to several distearoyl phosphoethanolamine lipids, thereby differing from conventional stealth liposomes where a PEG chain is attached to a single phospholipid. This composition was shown to increase liposomal stability, prolong the circulation half-life, improve the biodistribution profile and enhance the anticancer potency of a drug payload (doxorubicin hydrochloride).
© 2014 The Authors. Published by Elsevier B.V. This is an open access article under the CC BY-NC-SA 3.0 license (http://creativecommons.org/licenses/by/3.0/).

1. Introduction

Nanodelivery systems have been designed for the treatment of various diseases, such as cancer, diabetes, infections, allergy, asthma, and neurological disorders [1,2]. Indeed, nano-sized carriers have the potential to improve biopharmaceutical features, pharmacokinetic properties and the therapeutic efficacy of entrapped drugs [3]. A broad range of materials have been used for the fabrication of nanocarriers, including silicon and silica [4,5], lipids [6–8], polymers [9], surfactants [10,11], and metal [12]. Currently, there are several nanotherapeutics that are in clinical trials or have received approval, many of which are liposomal drugs [13,14]. The first liposomal formulation, Doxil, was approved by the Food and Drug Administration (FDA) in 1995 for the treatment of AIDS associated with Kaposi's sarcoma [15]. Since then, 14 liposomal drugs have been approved and 21 are enrolled in clinical trials [16–18]. Among these formulations several are approved for the treatment of cancer, including DepoCyt (liposomal cytarabine), DaunoXome (liposomal daunorubicin), Myocet (liposomal doxorubicin, approved in Europe and Canada), Doxil/Caelyx (liposomal doxorubicin), Sarcodoxome (liposomal doxorubicin), Marqibo (liposomal vincristine), and Lipusu (liposomal paclitaxel, approved in China) [18,19].

In order to improve the properties of liposomes and other drug delivery vehicles, polymers can be incorporated into these formulations [20,21]. This practice has opened up new opportunities in the field of pharmaceutical research and the design of novel polymer-based nanoparticles has been reported extensively in the literature [22–27]. Polyethylene glycol (PEG) is the most commonly used polymer in clinical practice [28]. The methoxy form of PEG, usually used for conjugation applications, has a single hydroxyl group that can be coupled with several entities, including small drugs, proteins, polymers and lipids [20]. Consequently, pegylation results in stealth shielding and increased circulation times [29]. In particular, the stealth effect is due to the formation of a dense hydrophilic barrier of PEG chains on the surface of the carrier, thereby reducing interactions with the reticular-endothelial system (RES). In addition, pegylation increases the hydrodynamic size of drug delivery systems and consequently decreases their clearance from the body [30,31]. Together these factors illustrate that the incorporation of PEG can improve the performance of nanovesicles. However, it should be noted that some forms of PEG-phospholipids might cause activation of the complement system and potentially cause pseudoallergic reactions [32].

* Corresponding author at: University "Magna Graecia" of Catanzaro, Building of Biosciences, Viale "S. Venuta", University Campus "S. Venuta", I-88100 Germaneto, Italy.
E-mail address: fresta@unicz.it (M. Fresta).
[1] These authors contributed equally.

http://dx.doi.org/10.1016/j.jconrel.2014.12.008
0168-3659/© 2014 The Authors. Published by Elsevier B.V. This is an open access article under the CC BY-NC-SA 3.0 license (http://creativecommons.org/licenses/by/3.0/).

The PEG coating of liposomes is generally achieved by using specific PEG-phospholipids, such as methoxy-PEG-distearoyl phosphoethanolamine (mPEG-DSPE), which can interact with the phospholipid bilayer through hydrophobic interactions. Liposomes surrounded by PEG chains are called stealth liposomes (SLs), as they are able to escape macrophage uptake [28,33]. Although this strategy increases the *in vivo* half-life of drug delivery systems [28], the beneficial effect of PEG shielding is limited. The limitation is due to the detachment of mPEG-phospholipid molecules from the surface of liposomes. This decrease in stability occurs when plasma proteins in the blood interact to the surface of nanoparticles, thereby, simultaneously modifying the distribution of PEG chains surrounding the surface of liposomes [34]. An additional limitation of stealth liposomes is the incomplete PEG shielding of the surface, leaving the carrier vulnerable to opsonization [35]. In this study, we have used novel PEG-dendron-phospholipids in order to create stable carrier systems, which we have termed super stealth liposomes (SSLs). The dendron structure acts as an anchor that enables several phospholipids to bind to a single PEG chain. This set-up enhances the interaction strength between mPEG-phospholipids and the phospholipid bilayer, thereby creating liposomes with higher stability. Throughout this study we have compared the performance of the SSLs to that of a conventional SL.

2. Materials and methods

2.1. Synthesis and characterization of mPEG-dendron derivates

PEG-dendron derivates were synthesized by conjugating mPEG-OH 5 kDa with nor-leucine (NLeu) or β-glutamic acid (βGlu) and further conjugating with DSPE. A pNO_2-phenyl activated PEG carbonate was prepared and purified by precipitation from diethyl ether and conjugation to NLeu or βGlu was performed in a borate buffer solution with a pH of 8. The intermediate, mPEG-NLeu-COOH or mPEG-βGlu, was extracted from the acidified solution with dichloromethane, concentrated to obtain a small volume, and recovered by precipitation in diethyl ether. The activation of these derivatives was carried out according to the standard procedure involving dicychlohexylcarbodiimide (DCC), and N-hydroxysuccinimide (NHS). For the synthesis of mPEG-βGlu$(βGlu)_2(DSPE)_4$, the reactions of βGlu coupling and activation *via* DCC/NHS was performed. The activated mPEG-NLeu-NHS, mPEG-βGlu$(NHS)_2$ or mPEG-βGlu$(βGlu)_2(NHS)_4$ was added to a DSPE chloroform solution and left to react overnight at 45 °C. The solvent was then removed under vacuum and the residue dissolved in water and dialysed against 50 mM NaCl and then against water using a membrane with a molecular cut-off of 100 kDa. The derivatives were recovered by freeze-drying. A further purification of mPEG-dendron derivates was carried out by dissolving the products in chloroform with equimolar amounts of stearoil chloride and triethylammine. The obtained reaction mixture was dropped into diethyl ether and the final products were recovered by filtration and dried under vacuum. The derivatives were characterized by ^{1}H-NMR spectroscopy and the Snyder assay [36].

2.2. Preparation of the SL and SSLs

The lipid composition for the SL was DPPC:Chol:mPEG2000-DSPE in a 6:3:0.5 molar ratio. In $SSL_{(1)}$ the PEG200-DSPE was interchanged for mPEG-NLeu-DSPE, in $SSL_{(2)}$ for mPEG-βGlu$(DSPE)_2$ and in $SSL_{(4)}$ for mPEG-βGlu$(βGlu)_2(DSPE)_4$. The lipids were dissolved in a round-bottom flask with 2 ml of a chloroform/methanol solution and the organic solvent was evaporated using a Rotavapor®. The liposomes were loaded with Dox through the use of a pH gradient remote loading procedure, as previously reported [37]. The SL and SSL formulations were then extruded through a stainless-steel extrusion device using polycarbonate membrane filters with 400 nm, 200 nm and 100 nm pores. Fluorescein DHPE (0.1% molar concentration) or ^{3}H[CHE] (1.25 μCi per formulation) were separately co-dissolved into lipid materials during the preparation procedure in order to obtain fluorescent- and ^{3}H[CHE]-mPEG-SSLs, respectively.

2.3. Purification and drug entrapment efficiency

Ultracentrifugation and gel filtration chromatography (GFC) were carried out in order to purify the SL and SSLs (from unstructured mPEG-dendron phospholipids and unentrapped drug) and to evaluate the drug entrapment efficiency. To avoid the dilution effect arising from the GFC purification procedure an ultracentrifugation method was also performed to further purify the formulations before *in vitro* and *in vivo* experiments. The amount of Dox entrapped within the SL and SSLs was evaluated according to a mathematical equation reported in the Supplementary material section.

2.4. Physicochemical characterization of the SL and SSLs

Dynamic light scattering was carried out to evaluate the physicochemical properties of the SL and SSLs [38]. Mean size, size distribution and zeta potential were evaluated using a Zetasizer Nano ZS apparatus (Malvern Instruments Ltd., Worchestershire, United Kingdom).

2.5. Evaluation of liposome stability by ITC and DLS

A conventional liposome, the SL and SSLs were subjected to Triton X-100 titration and monitored with ITC on a VP-ITC titration calorimeter (GE Healthcare, Uppsala, Sweden) [39] and by DLS. The titrant concentration at the solubilization boundary (C_D) was used to compare the stability of the vesicles. Further details about the stability measurements can be found in the Supplementary material section.

2.6. Fusion assays

FRET analysis was performed to evaluate vesicle fusion. A conventional liposome, the SL, and SSLs were formulated using energy donor and acceptor fluorescent probes prepared and co-incubated at 25 °C with a three-fold excess of unlabeled liposomes. $CaCl_2$ was added to the liposomal mixture to reach a final concentration of 10 mM. The fluorescence emission of the energy donor probe was measured using a spectrofluorometer (PerkinElmer LS-55, PerkinElmer, Monza (MB), Italy). A more detailed description of FRET analysis can be found in the Supplementary material section.

2.7. In vitro intracellular accumulation of Dox

CaCo-2 cells (1.5×10^5/ml) were seeded in a 24-well plate and incubated at 37 °C with 5% CO_2. After 24 h of incubation, cells were treated with free Dox, Dox/SL or Dox/SSLs (0.5 μM Dox) for various time periods. Cells were then washed with cold PBS buffer and lysed in 100 μl lysis buffer. The concentration of Dox was measured using a fluorescence spectrophotometer at 480 nm ($\lambda_{Excitation}$) and 575 nm ($\lambda_{Emission}$). The standard curve consisted of cellular lysates with scalar dilutions of Dox. The drug concentration was correlated to the amount of protein in the lysates. More details about the intracellular drug concentration measurements can be found in the Supporting material section.

2.8. Release profile of Dox from the SL and SSLs

The release of Dox from the SL and SSLs was investigated using a fluorescence dequenching assay according to a protocol reported in the Supplementary material section [40].

2.9. RP-HPLC method for Dox quantification

An HPLC apparatus was used to quantify the amount of Dox. The chromatographic separation was carried out using a reverse phase C18

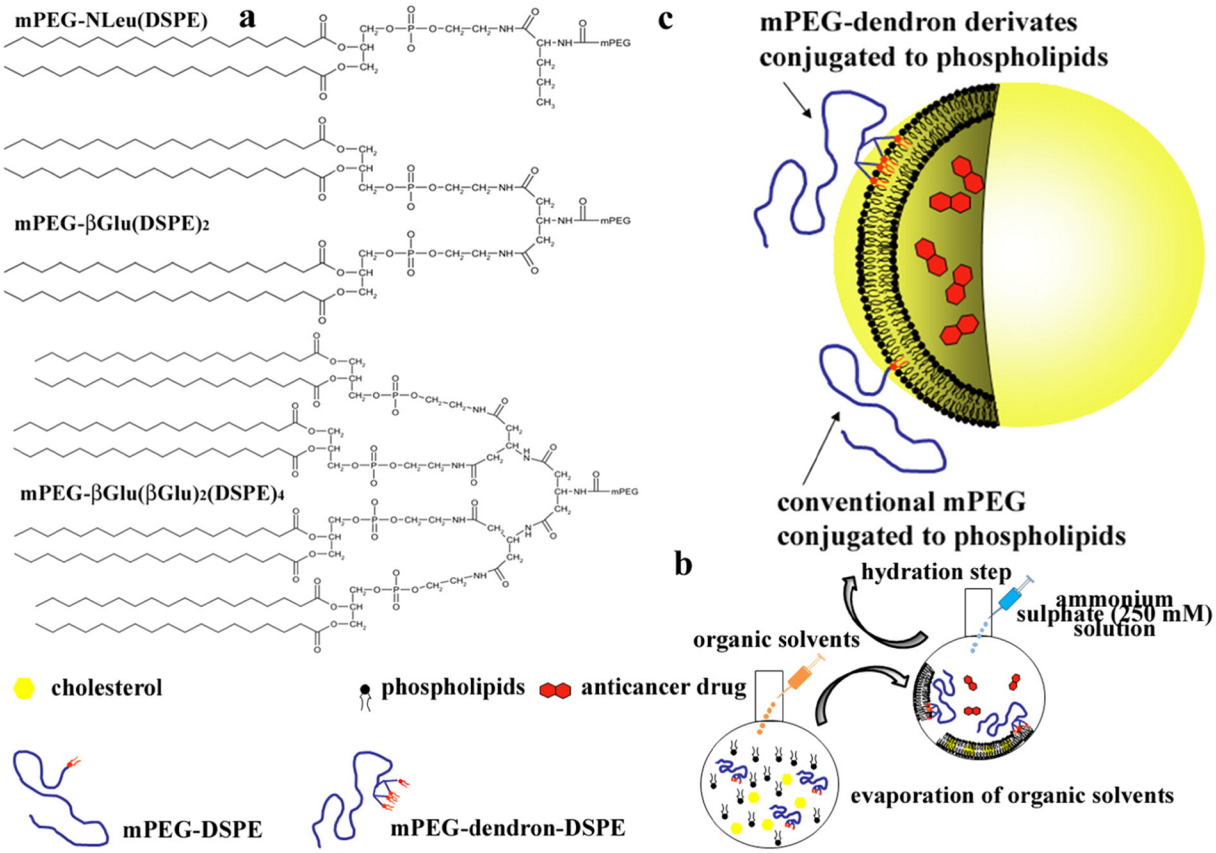

Fig. 1. Synthesis of pegylated dendron phospholipids for self-assembly of the stealth liposome (SL) and super stealth liposomes (SSLs) for anticancer therapy. a, The chemical structure of dendron phospholipids. b, Preparation procedure of SSLs. The formulations are prepared by using the following procedures: Thin layer evaporation, use of an ammonium sulfate pH gradient (250 mM) and extrusion through polycarbonate filter membranes (400 nm, 200 nm and 100 nm pores) (see the Materials and methods and Supplementary materials sections). c, Schematic representation of the SL and SSLs. In the SSLs the pegylated dendron derivates are attached to multiple lipid units. For clarity purposes the PEG chains have been depicted on the outer liposomal membrane. However, in reality, the chains are also present on the inner membrane. βGlu, β-glutamic acid; DSPE, distearoyl phosphoethanolamine; mPEG, methoxy polyethylene glycol; NLeu, Nor-leucin.

column and a mobile phase made up of 0.1% (v/v) trifluoroacetic acid in water and acetonitrile (25:75 v/v). The flow rate was 1.0 ml/min and the UV/Vis detector was set at 480 nm. An external calibration curve was used to quantify the samples. RP-HPLC was also used for the pharmacokinetic quantification of Dox. Chromatograms were acquired after drug extraction from plasma samples and interference between the drug and plasmatic protein was not observed.

2.10. Pharmacokinetic investigations

The Ethic Committee of the University of Padua approved the experiments (CEASA 24/2013) and all animals received care according to the DLGS 116/92 and in compliance with the "Guide for the Care and Use of Laboratory Animals". BALB/c mice (7–8 week old, 24–28 g) were used for the pharmacokinetic experiments. The mice received tail vein

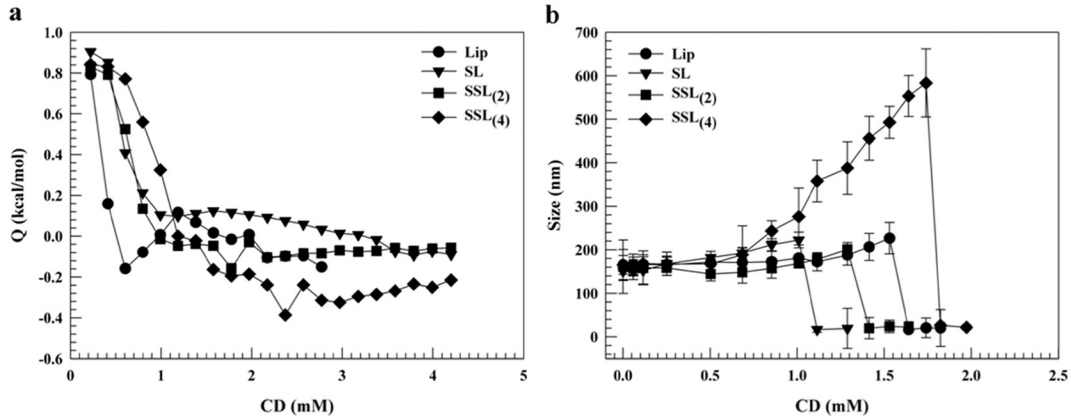

Fig. 2. Triton X-100 destabilization of liposomes. Evaluation of the stability of a conventional liposome (Lip), SL and SSLs using isothermal titration calorimetry (ITC) (a) and dynamic light scattering (DLS) (b). a, The integrated and normalized heat of reaction (Q) as a function of total detergent concentration in the ITC sample cell (C_D) was obtained by titrating a 3 mM (lipid equivalent) vesicle formulation with a 45 mM Triton X-100 solution. b, Vesicle size obtained by titrating a 3 mM (lipid equivalent) vesicle formulation with a 5 mM Triton X-100 solution. The data is reported as the mean of three different experiments ± standard deviation.

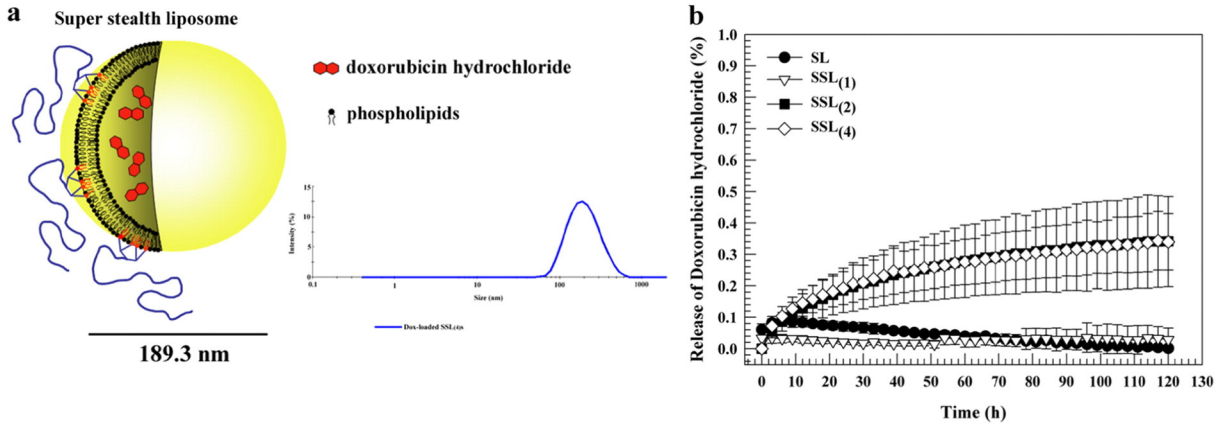

Fig. 3. Physicochemical characterization of $SSL_{(4)}$ self-assembled from mPEG-βGlu(βGlu)$_2$(DSPE)$_4$. a, Schematic representation of $SSL_{(4)}$ (mPEG-βGlu(βGlu)$_2$(DSPE)$_4$). b, Release profile of Dox from pegylated liposomes determined using a fluorescence dequenching method. The results are expressed as the ± standard deviation of three samples. Error bars, if not visible, are concealed behind the symbols.

injection of 150 μl of free Dox or Dox-SL/SSLs in isotonic 2.5 mM phosphate buffer solution at a pH of 7.4 (60 μg of Dox). At scheduled time points blood samples (~150 μl) were collected from the retro-orbital venous plexus by using heparin treated tubes and thereafter immediately centrifuged. A daunomicin solution was used as an internal standard. The samples were quantified by HPLC as reported elsewhere [41]. The data was analyzed by applying a two compartments model using the PKSolver program.

2.11. Biodistribution of the SL and SSLs

Biodistribution analysis was carried out in BALB/c mice (7–8 week old, 24–28 g). Mice were divided into four groups and injected through the tail vein with ^{3}H[CHE]-SL/SSLs (200 μl, 0.5 μCi of ^{3}H[CHE]). At different time points (1, 8, 16 and 24 h) blood was collected from the retro-orbital plexus and mice were then sacrificed. The heart, lungs, liver, spleen and kidneys were surgically harvested and the tissue weights were recorded (Table S2). The organs and blood were digested with a quaternary ammonium hydroxide solution, acidified with sulfuric acid (1 N) and quantified using a β scintillation counter. The biodistribution was expressed as the percentage of injected dose per gram of tissue.

2.12. Stability of ^{3}H[CHE]-SL/SSL in serum

^{3}H[CHE]-SL/SSLs were used to evaluate the liposomal stability. Liposomes diluted in PBS buffer solution (500 μl, pH 7.4) were incubated with bovine serum (500 μl). The samples were maintained under continuous stirring at 37 °C and 50 μl of solution was withdrawn at different time points. The collected solutions were spun down with Bio-Gel A-15 spin columns and analyzed using a β-scintillation counter.

2.13. In vitro anticancer activity

The anticancer activity of the free drug and Dox-SL/SSLs was assayed in CaCo-2 cells using the MTT viability test. Different doses and incubation times were evaluated. Cells were treated with 200 μl of fresh medium (control), empty SSLs (blank control) or different concentrations of free drug and Dox-SL/SSLs. The anticancer activity (cell viability percentage) was evaluated after 24 h, 48 h or 72 h of incubation and quantified with a UV spectrophotometer micro plate reader and the absorption was measured at a wavelength of 570 nm.

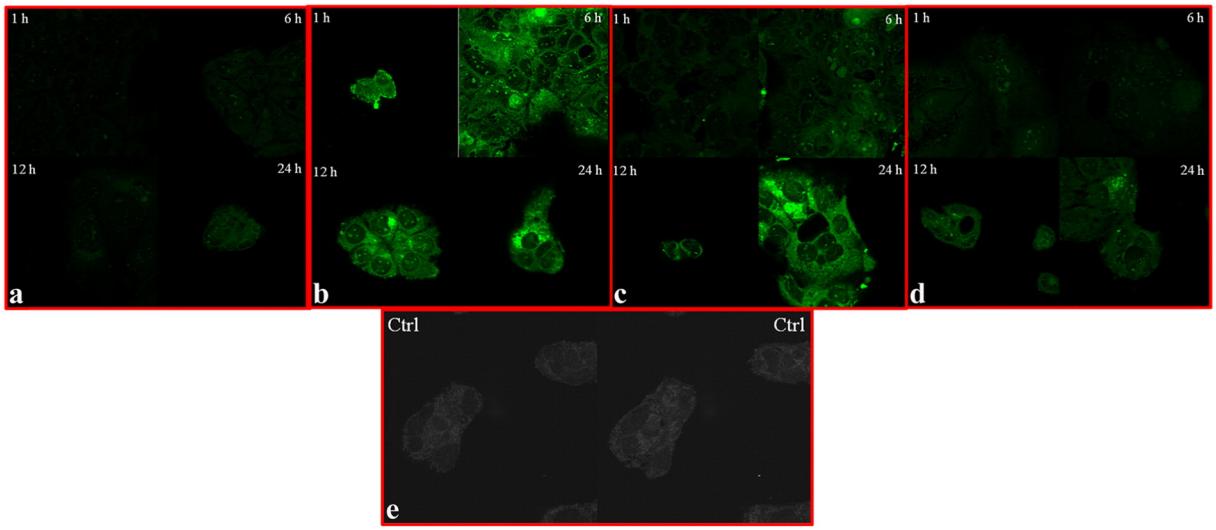

Fig. 4. Confocal laser scanning micrographs of CaCo-2 cells incubated with fluorescein labeled SL and SSLs. CaCo-2 cells were treated with fluorescent SL or SSLs and incubated for different time periods (1 h, 6 h, 12 h and 24 h). a, SL. b, $SSL_{(1)}$. c, $SSL_{(2)}$. d, $SSL_{(4)}$. e, Control (untreated CaCo-2 cells).

2.14. Confocal laser scanning microscopy (CLSM)

CLSM was carried out on CaCo-2 cells by using fluorescein-DHPE as a labeling agent. Cells were seeded in 6-well plates with glass slides (6.0×10^4 cells/ml) and incubated for 24 h. The cells were then treated with fluorescent SL and SSLs and incubated for different time periods (1 h, 3 h, 6 h, 12 h and 24 h). At the end of the incubation period excess fluorescein-labeled vesicles were removed with PBS buffer solution (pH 7.4) and cells were fixed with cooled ethanol solution. Excess ethanol was removed and the cells were further washed with PBS buffer solution (pH 7.4). 200 μl of cellular suspension was loaded onto a glass holder and fixed with a 95% (v/v) ethanol solution. Quantification was performed with a Leica TCS SP2 MP confocal laser scanning microscopy.

3. Results and discussion

3.1. Design, preparation and physicochemical characterization of SSLs

We have designed a series of mPEG-dendron-phospholipid derivatives that have been synthesized in-house. The hydroxyl end of an mPEG chain was attached to a dendron anchor, consisting of N leucin (NLeu), β-glutamic acid (βGlu) or βGlu(βGlu)$_2$. At the opposite side the anchor was conjugated to one, two or four DSPE units, resulting in the following constructs: SSL$_{(1)}$ (mPEG-NLeu(DSPE)), SSL$_{(2)}$ (mPEG-βGlu(DSPE)$_2$) and SSL$_{(4)}$ (mPEG-βGlu(βGlu)$_2$(DSPE)$_4$) (Fig. 1a). ^{1}H-NMR spectroscopy was used to confirm the ratio between the polymer and the DSPE lipids (Supplementary Fig. S1). Measurements at the critical concentration for aggregation (CCA) show that the dimensions of the lipid derivatives remain small (Supplementary Fig. S2). This result demonstrates the lack of aggregates or micelles, which increases the chance that the lipid derivatives will be successfully integrated within the phospholipid bilayer. The dendron structures were then self-assembled with other lipid components to obtain SSLs. The mean size of the SSLs was ~160 nm and the narrow size distribution was below 0.2 (Supplementary Table S1). All SSLs, except SSL$_{(1)}$, had a greater negative zeta potential value than that of PEGylated liposomes (Supplementary Table S1). This finding was expected as SSL$_{(1)}$ derivatives only have one lipid unit attached to the PEG chain, resembling conventional PEGylated liposomes. The zeta potential data was measured as a function of electrophoretic mobility (Supplementary Table S1).

The SSLs were further analyzed using a PEG enzyme-linked immunosorbent assay (ELISA) kit to evaluate potential differences in the concentration of PEG on the vesicular surface. The order from highest to lowest PEG content was the following: SSL$_{(4)}$ > SSL$_{(2)}$ > SL (Supplementary Fig. S3). Higher amounts of PEG on the surface of SSL$_{(4)}$ may be attributable to the βGlu(βGlu)$_2$ spacer, which strongly anchors the PEG moieties to four phospholipid units.

Isothermal titration calorimetry (ITC) and dynamic light scattering (DLS) experiments were performed to evaluate the stability of a conventional liposome (Lip), a SL and SSLs exposed to Triton X-100 titration. ITC demonstrated that the Q_D (kcal/mol) values drop abruptly at the solubilization boundary, which separates the bilayer/micelle coexistence range from the micelle range (Fig. 2a). The order of stability from the highest to the lowest was the following: SSL$_4$ > SSL$_2$ > SL > Lip. The same order of stability was observed when the titration was performed in conjunction with DLS, which measures the size of colloidal vesicles (Fig. 2b). In particular, at higher concentrations of Triton-X 100, the size of SSL$_{(4)}$ increased, while the other liposomes were disrupted. This observation indicates that despite the change in size, SSL$_{(4)}$ is able to withstand the intercalation of surfactant into the lipid bilayer. The evaluation of the polydispersity index (PDI) as a function of the Triton X-100 concentration revealed that SSL$_{(4)}$ displayed an abrupt increase in PDI (>0.4) at a higher surfactant concentration as compared to the other liposomes (Supplementary Fig. S4), providing further evidence that SSL$_{(4)}$ exhibits improved stability. When comparing ITC and DLS, slight differences were observed in the detergent concentration (C_D) that was required for solubilization. This discrepancy may be ascribed to the use of different protocols, *e.g.* continuous mixing during ITC and varying time intervals between detergent additions. Fluorescence resonance energy transfer (FRET) analysis was performed to measure liposomal fusion, which is an indication of liposomal instability. The results suggest that the conventional liposome underwent fusion, while the structural integrity of the stealth liposome and the super stealth liposomes was maintained (Supplementary Fig. S5). The SSL$_{(4)}$ and SSL$_{(2)}$ displayed slightly higher stability compared to the SL (Supplementary Fig. S5).

The SSLs were evaluated as anticancer drug carriers (Fig. 1b,c) by encapsulating doxorubicin hydrochloride (Dox) in the liposomal core. All

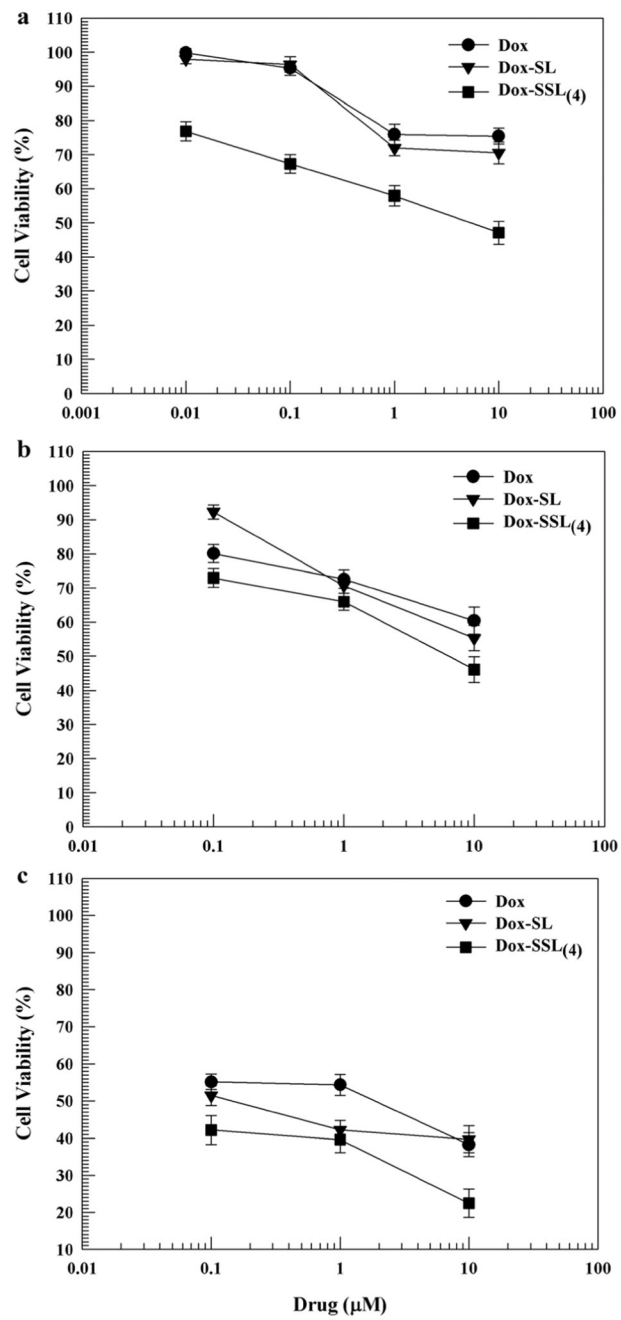

Fig. 5. *In vitro* dose-dependent antitumor effects of free doxorubicin hydrochloride (Dox) and Dox loaded SL and SSL$_{(4)}$ in CaCo-2 cells. a, 24 h incubation. b, 48 h incubation. c, 72 h incubation. Legend symbols: Free Dox (●); Dox-SL (▼), Dox-SSL$_{(4)}$ (■). Untreated cells were used as controls (100% viability). The results are expressed as the average of three different experiments ± standard deviation. Error bars, if not visible, are concealed under the symbols.

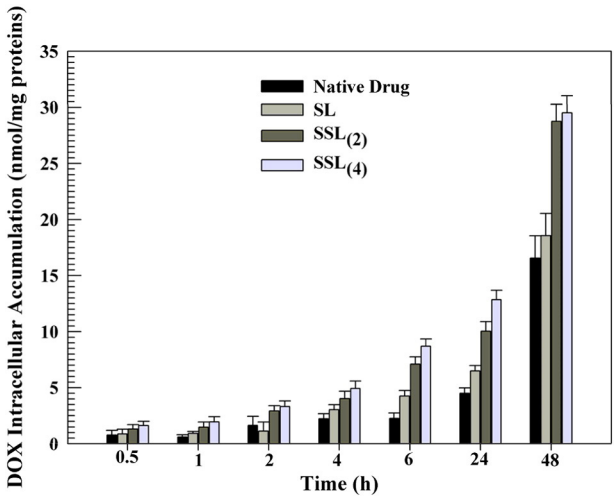

Fig. 6. Intracellular accumulation of free DOX, DOX-SL, DOX-$SSL_{(2)}$, DOX-$SSL_{(4)}$ in CaCo-2 cells. The experiments were carried out at 37 °C at a drug concentration of 0.5 μM. Each bar represents the average value of three different experiments + standard deviation.

Dox-SSL formulations had a diameter of less than 200 nm, making them suitable for systemic administration and drug delivery (Fig. 3 a,c and Supplementary Table S1). In particular, the small size allows the carrier to move through endothelial fenestrations (~200 nm) in neo-formed tumor vasculature [42]. The mean size of the Dox-SSLs was similar to that of empty SSLs (~160) (Fig. 3a,b), with the exception of $SSL_{(4)}$ (~189 nm) (Supplementary Table S1). The zeta potential values also remained unchanged after the addition of Dox (Supplementary Table S1). In all of the SSLs the entrapment efficiency of Dox was higher than 80% (Supplementary Fig. S6). Indeed, the presence of a transmembrane pH gradient promoted the arrangement of the drug into the aqueous compartment, forming a gel-like structure and avoiding leakage from the vesicular bilayer [43]. All liposomal formulations displayed a slow release of Dox, *i.e.* lower than 0.5% after 2 h of incubation (Fig. 3b). This finding is in agreement with previous observations of conventional liposomes (Lip) and SL [43].

Table 1
Main pharmacokinetic parameters of free Dox, the SL and SSLs after intravenous injection in Balb/C mice (50–60 days old, 24–28 g).

Formulations	$t_{½}$ α (min)[a]	$t_{½}$ β (min)[b]	AUC 0–∞ (μg/ml·min)	Vss (ml)	Cl (ml/min)[c]
Free Dox[d]	2.7	154.2	7.3	1740.3	83.7
Dox[d]-SL	4.7	151.6	2705.8	4.3	0.103
Dox[d]-$SSL_{(1)}$	3.92	144.5	2403.1	4.0	0.102
Dox[d]-$SSL_{(2)}$	8.97	633.5	7063.8	7.5	0.113
Dox[d]-$SSL_{(4)}$	29.0	888.3	20424.5	3.4	0.016

[a] Distribution half-life.
[b] Post-distribution half-life.
[c] Cumulative clearance.
[d] Doxorubicin hydrochloride.

3.2. In vitro and in vivo investigations of SSLs

The internalization of liposomes in CaCo-2 cells was evaluated by including a fluorescein-conjugated lipid in the liposomal bilayer. The results show that SSLs accumulate in higher amounts inside the cells, in comparison to the SL (Fig. 4).

Although hydrophilic polymers are known to decrease the interactions between liposomes and biological substrates, other factors should also be considered in order to explain the improved intracellular uptake of SSLs. Firstly, interactions between liposomes and cells also depend on the physicochemical features and lipid compositions of vesicles [44], *e.g.* negatively charged liposomes have increased cellular uptake *in vitro* and *in vivo* in comparison to neutral liposomes [45,46]. Thus, the increased cellular internalization could be attributable to the fact that SSLs are more anionic than SL (Supplementary Table S1). Secondly, the improved intracellular uptake of SSLs may be due to interactions between the dendron anchors and the cell membrane. For instance, it is possible that some of the glutamic acid dendron derivatives are able to interact with glutamate receptors on the surface of cancer cells, thereby triggering internalization. Thirdly, vesicle size also plays a role

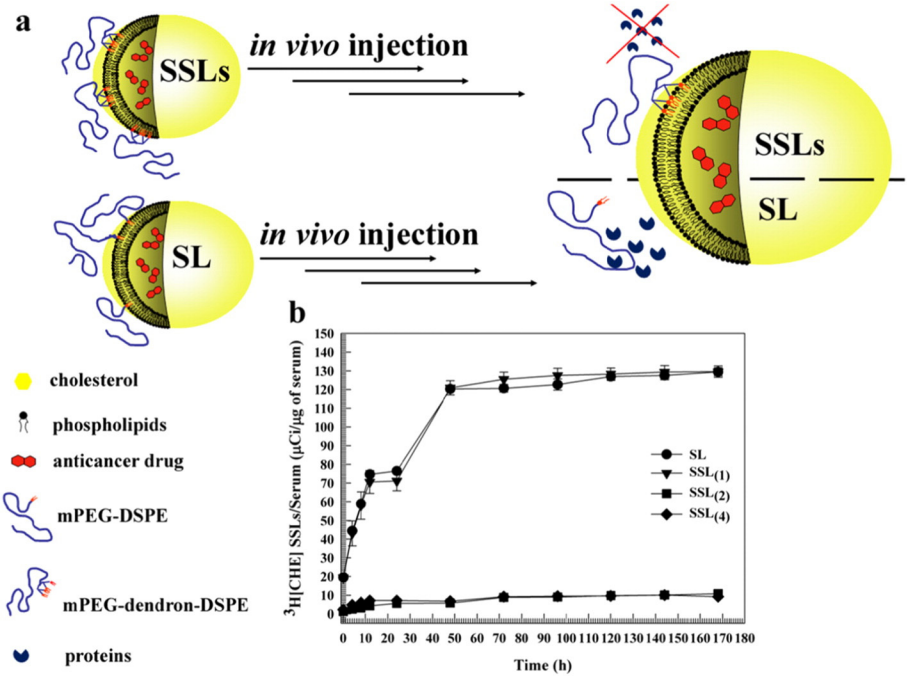

Fig. 7. Serum incubation of SL and SSLs. a, Schematic description of the effect of serum proteins on lipid detachment from the liposomal bilayer. b, Stability of SSLs in serum. The leakage of ^{3}[H]CHE from the SL and SSLs was used as a measurement for stability. Legend symbols: SL (●), $SSL_{(1)}$ (▼); $SSL_{(2)}$ (■) and $SSL_{(4)}$ (♦). The results are the average of three different experiments ± standard deviation. Error bars, if not visible, are concealed under the symbols.

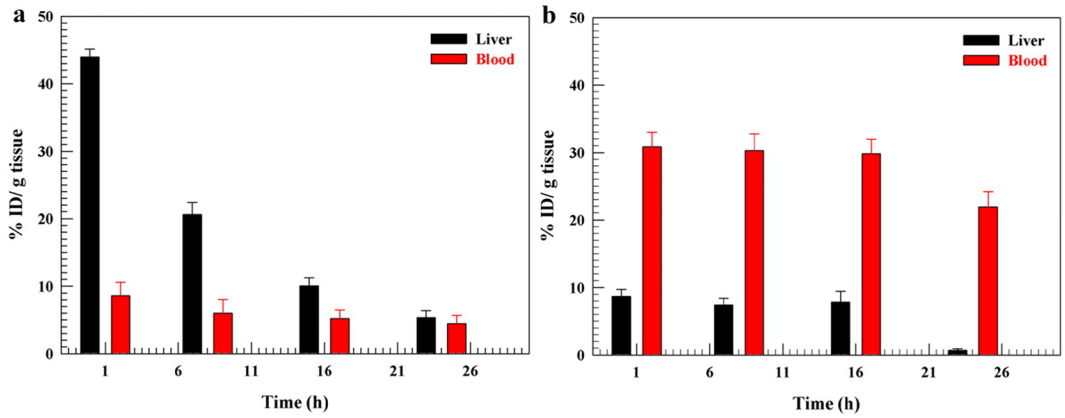

Fig. 8. Biodistribution of ^{3}[H]CHE-labeled SL and $SSL_{(4)}$ after intravenous injection in Balb/C mice. ^{3}[H]CHE-labeled SL and $SSL_{(4)}$ (200 μl, 0.5 μCi of ^{3}[H]CHE) was injected through the tail vein and quantified at different incubation times (1, 8, 16 and 24 h). Blood was collected and mice were sacrificed. The amount of liposomes in the blood and liver was determined a, SL. b, $SSL_{(4)}$. Results are the average of three experiments ± standard deviation. ID, injected dose.

in the interactions between nanoparticles and living cells [47]. Indeed, the sizes of SSLs differed slightly from that of SL, potentially affecting intracellular uptake (Supplementary Table S1). As can be seen in Fig. 4, $SSL_{(4)}$ displayed lower intracellular uptake in comparison to $SSL_{(1)}$ and $SSL_{(2)}$. This effect may be dependent on the conformation of PEG, *i.e.* it is possible that the PEG chains on $SSL_{(4)}$ are in a brush conformation, which partially prevents endocytosis [48].

Safety and biocompatibility of mPEG-dendron derivates alone or self-assembled into SSLs were tested using human keratinocyte cells (NCTC 2544), as previously reported in the literature [49]. The cells that were incubated with the dendron structures had a viability of over 90% after 72 h (Supplementary Fig. S7) and showed normal morphology (Supplementary Fig. S8). Cells subjected to drug-free SSLs also showed high cell viability, which was similar to that of the empty SL (Supplementary Fig. S9).

The Dox-SSLs were tested in CaCo-2 cells to evaluate the anticancer activity and the efficacy was compared to that of Dox-SL and free Dox. Dose-dependent and time-dependent experiments were performed (Fig. 5 and Supplementary Figure S10). When Dox was loaded into $SSL_{(4)}$ and $SSL_{(2)}$ it showed higher toxicity (~57 % and ~59 % cell viability) than when loaded into the SL (~92%) or when used as a free drug (~94%) (0.01 μM, 72 h) (Fig. 5 and Supplementary Fig. S10). At the lowest Dox concentration (0.01 μM) only $SSL_{(4)}$ showed a significant reduction in cell viability (~77%, 24 h and 48 h) (Supplementary Fig. S10a,b). In order to achieve a similar reduction of cell viability with the SL or the free drug a 1000-fold higher dose of drug was needed (Supplementary Fig. S10a). The intracellular uptake of Dox, Dox-SL, Dox-$SSL_{(2)}$ and Dox-$SSL_{(4)}$ was measured in CaCo-2 cells. The levels of intracellular Dox were higher when using $SSL_{(2)}$ and $SSL_{(4)}$ in comparison to SL and native drug (Fig. 6).

Since the properties of liposomes can change considerably in an *in vivo* environment [50], the stability of SSLs was evaluated in serum. In particular, the integrity of liposomes was measured by including ^{3}H[CHE] in the bilayer. The release of ^{3}[H]CHE can be used as an indirect measurement of liposome stability, since it is a nonexchangeable lipid marker. In fact, ^{3}[H] CHE cannot be released from the lipid bilayer without modifying the liposome structure, which typically entails the detachment of phospholipids. The results show that there is a large difference in the stability of SL and $SSL_{(1)}$ in comparison to $SSL_{(2)}$ and $SSL_{(4)}$ (Fig. 7a,b). After 180 h SL and $SSL_{(1)}$ had ~130 μCi ^{3}H[CHE] per μg serum, while $SSL_{(2)}$ and $SSL_{(4)}$ had ~10 μCi ^{3}H[CHE] per μg serum (Fig. 7b).

Furthermore, $SSL_{(2)}$ and $SSL_{(4)}$ in comparison to SL and $SSL_{(1)}$, significantly improved the biopharmaceutical features and pharmacokinetic profile of Dox after *in vivo* injection (Supplementary Fig. S11 and S12 and Table 1). Especially $SSL_{(4)}$ showed a 6.2-fold increase in the distribution half life ($t_{½}$ α) and 5.86-fold increase in the post-distribution half life ($t_{½}$ β) of Dox, respectively and a 7.6-fold increase in the area under the plasma concentration–time curve (AUC) value in comparison to SL (Supplementary Fig. S12 and Table 1). This supports the *in vitro* findings and suggests that the stability of SSLs is also greater than that of SL in an *in vivo* environment. Moreover the biodistribution of SL and SSLs was measured in a time dependent manner (1, 8, 16 and 24 h after i.v. administration) in six different organs, including the circulatory system. We show that SSLs are present in the blood in greater amounts and for longer times and accumulate at a lower extent in the RES (Fig. 8a,b and Supplementary Fig. S11 a,b). After 1 h the percentage of injected dose (ID) per gram of tissue in the liver was ~44% with SL vs ~9% with $SSL_{(4)}$, while the values for the blood were 9% with SL and 30% with $SSL_{(4)}$ (Fig. 8).

4. Conclusions

The following study proposes the use of mPEG-dendron-phospholipids to improve biopharmaceutical and pharmacokinetic features of liposomes. We have synthesized novel mPEG derivates that self assemble into super stealth liposomes. The dendron structure results in an increase of the phospholipid/PEG attachment ratio and consequently ensures a more stable interaction between the PEG chains and the vesicular surface. The stable interaction inhibits the rapid detachment of PEG in the circulatory system. Indeed, Triton X-100 titration showed that the SSLs were more resistant to solubilization by a surfactant. Likewise, the SSLs demonstrated less detachment of lipids from the liposomal bilayer in the presence of serum proteins. The pharmacokinetic profile of SSLs, particularly $SSL_{(4)}$, exceeds that of conventional PEGylated liposomes. SSLs have increased stability, prolonged circulation half-life, and lower uptake in RES organs in comparison to the stealth liposome. Furthermore, *in vitro* studies suggest that SSLs have low toxicity and high intracellular uptake. Cell culture studies also demonstrate that Dox loaded within an SSL outperforms both Dox-SL and free Dox. Notably, the Dox dose used with SSLs can be up to 1000-fold lower than conventional stealth liposomes to achieve the same anticancer activity *in vitro*. The reason for the improved therapeutic efficacy could be a combination of increased intracellular uptake and drug release of SSLs. The obtained results demonstrate that SSLs may have the potential to greatly improve conventional cancer treatment by enhancing drug delivery and antitumor efficacy.

Conflict of interest

GF and OS have a patent involving super stealth liposomes (WO 2010/143218 A1). The other authors declare no competing financial interest.

Acknowledgments

This paper was financially supported by grants from the Italian Ministry of University and Research (PRIN 2006030353_005; EX60% 60A04-1870/13), and by a grant from the PON a3_00359 (IRC-FSH) Interregional Research Center for Food Safety & Health. The authors are very grateful to Dr. Nicola Costa (Department of Health Sciences, University of Catanzaro) for his valuable support and technical assistance with the biodistribution experiments and to Dr. Elena Canato (Pharmaceutical and Pharmacological Department, University of Padova) for her valuable support and assistance in the release experiments.

Appendix A. Supplementary data

Supplementary data to this article can be found online at http://dx.doi.org/10.1016/j.jconrel.2014.12.008.

References

[1] V. Wagner, A. Dullaart, A.K. Bock, A. Zweck, The emerging nanomedicine landscape, Nat. Biotechnol. 24 (2006) 1211–1217.
[2] R.A. Petros, J.M. DeSimone, Strategies in the design of nanoparticles for therapeutic applications, Nat. Rev. Drug Discov. 9 (2010) 615–627.
[3] D.A. Scheinberg, C.H. Villa, F.E. Escorcia, M.R. McDevitt, Conscripts of the infinite armada: systemic cancer therapy using nanomaterials, Nat. Rev. Clin. Oncol. 7 (2010) 266–276.
[4] J. Shen, R. Xu, J. Mai, H.C. Kim, X. Guo, G. Qin, Y. Yang, J. Wolfram, C. Mu, X. Xia, J. Gu, X. Liu, Z.W. Mao, M. Ferrari, H. Shen, High capacity nanoporous silicon carrier for systemic delivery of gene silencing therapeutics, ACS Nano 7 (2013) 9867–9880.
[5] J. Shen, H.C. Kim, H. Su, F. Wang, J. Wolfram, D. Kirui, J. Mai, C. Mu, Z. Mao, H. Shen, Cyclodextrin and polyethylenimine functionalized mesoporous silica nanoparticles for delivery of siRNA cancer therapeutics, Theranostics 4 (2014) 487–497.
[6] J. Wolfram, K. Suri, Y. Huang, R. Molinaro, C. Borsoi, B. Scott, K. Boom, D. Paolino, M. Fresta, J. Wang, M. Ferrari, C. Celia, H. Shen, Evaluation of anticancer activity of celastrol liposomes in prostate cancer cells, J. Microencapsul. 31 (2014) 501–507.
[7] C. Celia, E. Trapasso, M. Locatelli, M. Navarra, C.A. Ventura, J. Wolfram, M. Carafa, V.M. Morittu, D. Britti, L. Di Marzio, D. Paolino, Anticancer activity of liposomal bergamot essential oil (BEO) on human neuroblastoma cells, Colloids Surf. B: Biointerfaces (2013) 548–553.
[8] D. Paolino, D. Cosco, M. Gaspari, M. Celano, J. Wolfram, P. Voce, E. Puxeddu, S. Filetti, C. Celia, M. Ferrari, D. Russo, M. Fresta, Targeting the thyroid gland with thyroid stimulating hormone (TSH)-nanoliposomes, Biomaterials 35 (2014) 7101–7109.
[9] R. Molinaro, J. Wolfram, C. Federico, F. Cilurzo, L. Di Marzio, C.A. Ventura, M. Carafa, C. Celia, M. Fresta, Polyethylenimine and chitosan carriers for the delivery of RNA interference effectors, Expert Opin. Drug Deliv. 10 (2013) 1653–1668.
[10] L. Di Marzio, S. Esposito, F. Rinaldi, C. Marianecci, M. Carafa, Polysorbate 20 vesicles as oral delivery system: in vitro characterization, Colloids Surf. B: Biointerfaces 104 (2013) 200–206.
[11] L. Di Marzio, C. Marianecci, M. Petrone, F. Rinaldi, M. Carafa, Novel pH-sensitive nonionic surfactant vesicles: comparison between Tween 21 and Tween 20, Colloids Surf. B: Biointerfaces 82 (2011) 18–24.
[12] J. Shen, H.C. Kim, C. Mu, E. Gentile, J. Mai, J. Wolfram, L. Ji, M. Ferrari, Z. Mao, H. Shen, Multifunctional gold nanorods for siRNA gene silencing and photothermal therapy, Adv. Healthc. Mater. 3 (2014) 1629–1637.
[13] L. Zhang, F.X. Gu, J.M. Chan, A.Z. Wang, R.S. Langer, O.C. Farokhzad, Nanoparticles in medicine: therapeutic applications and developments, Clin. Pharmacol. Ther. 83 (2008) 761–769.
[14] A.G. Cattaneo, R. Gornati, E. Sabbioni, M. Chiriva-Internati, E. Cobos, M.R. Jenkins, G. Bernardini, Nanotechnology and human health: risks and benefits, J. Appl. Toxicol. 30 (2010) 730–744.
[15] D.W. Northfelt, B.J. Dezube, J.A. Thommes, B.J. Miller, M.A. Fischl, A. Friedman-Kien, L.D. Kaplan, C.Du. Mond, R.D. Mamelok, D.H. Henry, Pegylated-liposomal doxorubicin versus doxorubicin, bleomycin, and vincristine in the treatment of AIDS-related Kaposi's sarcoma: results of a randomized phase III clinical trial, J. Clin. Oncol. 16 (1998) 2445–2451.
[16] H.I. Chang, M.K. Yeh, Clinical development of liposome-based drugs: formulation, characterization, and therapeutic efficacy, Int. J. Nanomedicine 7 (2012) 49–60.
[17] S. Koudelka, J. Turanek, Liposomal paclitaxel formulations, J. Control. Release 163 (2012) 322–334.
[18] J.A. Silverman, S.R. Deitcher, Marqibo(R) (vincristine sulfate liposome injection) improves the pharmacokinetics and pharmacodynamics of vincristine, Cancer Chemother. Pharmacol. 71 (2013) 555–564.
[19] E. Gentile, F. Cilurzo, L. Di Marzio, M. Carafa, C.A. Ventura, J. Wolfram, D. Paolino, C. Celia, Liposomal chemotherapeutics, Future Oncol. 9 (2013) 1849–1859.
[20] J.A. Hubbell, A. Chilkoti, Chemistry, nanomaterials for drug delivery, Science 337 (2012) 303–305.
[21] S. Mitragotri, J. Lahann, Physical approaches to biomaterial design, Nat. Mater. 8 (2009) 15–23.
[22] S. Aryal, C.M. Hu, L. Zhang, Polymer–cisplatin conjugate nanoparticles for acid-responsive drug delivery, ACS Nano 4 (2010) 251–258.
[23] R.H. Fang, S. Aryal, C.M. Hu, L. Zhang, Quick synthesis of lipid–polymer hybrid nanoparticles with low polydispersity using a single-step sonication method, Langmuir 26 (2010) 16958–16962.
[24] S. Aryal, C.M. Hu, L. Zhang, Synthesis of ptsome: a platinum-based liposome-like nanostructure, Chem. Commun. (Camb.) 48 (2012) 2630–2632.
[25] D. Paolino, D. Cosco, M. Licciardi, G. Giammona, M. Fresta, G. Cavallaro, Polyaspartylhydrazide copolymer-based supramolecular vesicular aggregates as delivery devices for anticancer drugs, Biomacromolecules 9 (2008) 1117–1130.
[26] M. Licciardi, D. Paolino, C. Celia, G. Giammona, G. Cavallaro, M. Fresta, Folate-targeted supramolecular vesicular aggregates based on polyaspartyl-hydrazide copolymers for the selective delivery of antitumoral drugs, Biomaterials 31 (2010) 7340–7354.
[27] D. Paolino, M. Licciardi, C. Celia, G. Giammona, M. Fresta, G. Cavallaro, Folate-targeted supramolecular vesicular aggregates as a new frontier for effective anticancer treatment in in vivo model, Eur. J. Pharm. Biopharm. 82 (2012) 94–102.
[28] G. Pasut, F.M. Veronese, PEGylation for improving the effectiveness of therapeutic biomolecules, Drugs Today (Barc.) 45 (2009) 687–695.
[29] G. Pasut, F.M. Veronese, State of the art in PEGylation: the great versatility achieved after forty years of research, J. Control. Release 161 (2012) 461–472.
[30] A. Jain, S.K. Jain, PEGylation: an approach for drug delivery. A review, Crit. Rev. Ther. Drug Carrier Syst. 25 (2008) 403–447.
[31] J.M. Harris, R.B. Chess, Effect of pegylation on pharmaceuticals, Nat. Rev. Drug Discov. 2 (2003) 214–221.
[32] S.M. Moghimi, A.J. Andersen, S.H. Hashemi, B. Lettiero, D. Ahmadvand, A.C. Hunter, T.L. Andresen, I. Hamad, J. Szebeni, Complement activation cascade triggered by PEG-PL engineered nanomedicines and carbon nanotubes: the challenges ahead, J. Control. Release 146 (2010) 175–181.
[33] V.P. Torchilin, Recent advances with liposomes as pharmaceutical carriers, Nat. Rev. Drug Discov. 4 (2005) 145–160.
[34] M.J. Parr, S.M. Ansell, L.S. Choi, P.R. Cullis, Factors influencing the retention and chemical stability of poly(ethylene glycol)-lipid conjugates incorporated into large unilamellar vesicles, Biochim. Biophys. Acta 1195 (1994) 21–30.
[35] S.D. Li, L. Huang, Stealth nanoparticles: high density but sheddable PEG is a key for tumor targeting, J. Control. Release 145 (2010) 178–181.
[36] S.L. Snyder, P.Z. Sobocinski, An improved 2,4,6-trinitrobenzenesulfonic acid method for the determination of amines, Anal. Biochem. 64 (1975) 284–288.
[37] C. Celia, N. Malara, R. Terracciano, D. Cosco, D. Paolino, M. Fresta, R. Savino, Liposomal delivery improves the growth-inhibitory and apoptotic activity of low doses of gemcitabine in multiple myeloma cancer cells, Nanomedicine 4 (2008) 155–166.
[38] D. Paolino, D. Cosco, L. Racanicchi, E. Trapasso, C. Celia, M. Iannone, E. Puxeddu, G. Costante, S. Filetti, D. Russo, M. Fresta, Gemcitabine-loaded PEGylated unilamellar liposomes vs GEMZAR: biodistribution, pharmacokinetic features and in vivo antitumor activity, J. Control. Release 144 (2010) 144–150.
[39] O.O. Krylova, N. Jahnke, S. Keller, Membrane solubilisation and reconstitution by octylglucoside: comparison of synthetic lipid and natural lipid extract by isothermal titration calorimetry, Biophys. Chem. 150 (2010) 105–111.
[40] T. Ishida, M.J. Kirchmeier, E.H. Moase, S. Zalipsky, T.M. Allen, Targeted delivery and triggered release of liposomal doxorubicin enhances cytotoxicity against human B lymphoma cells, Biochim. Biophys. Acta 1515 (2001) 144–158.
[41] G. Pasut, F. Greco, A. Mero, R. Mendichi, C. Fante, R.J. Green, F.M. Veronese, Polymer-drug conjugates for combination anticancer therapy: investigating the mechanism of action, J. Med. Chem. 52 (2009) 6499–6502.
[42] D.C. Drummond, O. Meyer, K. Hong, D.B. Kirpotin, D. Papahadjopoulos, Optimizing liposomes for delivery of chemotherapeutic agents to solid tumors, Pharmacol. Rev. 51 (1999) 691–743.
[43] A. Fritze, F. Hens, A. Kimpfler, R. Schubert, R. Peschka-Suss, Remote loading of doxorubicin into liposomes driven by a transmembrane phosphate gradient, Biochim. Biophys. Acta 1758 (2006) 1633–1640.
[44] M.G. Calvagno, C. Celia, D. Paolino, D. Cosco, M. Iannone, F. Castelli, P. Doldo, M. Fresta, Effects of lipid composition and preparation conditions on physical–chemical properties, technological parameters and in vitro biological activity of gemcitabine-loaded liposomes, Curr. Drug Deliv. 4 (2007) 89–101.
[45] T.M. Allen, P. Williamson, R.A. Schlegel, Phosphatidylserine as a determinant of reticuloendothelial recognition of liposome models of the erythrocyte surface, Proc. Natl. Acad. Sci. U. S. A. 85 (1988) 8067–8071.
[46] J.H. Senior, Fate and behavior of liposomes in vivo: a review of controlling factors, Crit. Rev. Ther. Drug Carrier Syst. 3 (1987) 123–193.
[47] W.K. Chang, Y.J. Tai, C.H. Chiang, C.S. Hu, P.D. Hong, M.Y. Yeh, The comparison of protein-entrapped liposomes and lipoparticles: preparation, characterization, and efficacy of cellular uptake, Int. J. Nanomedicine 6 (2011) 2403–2417.
[48] R. Bartucci, M. Pantusa, D. Marsh, L. Sportelli, Interaction of human serum albumin with membranes containing polymer-grafted lipids: spin-label ESR studies in the mushroom and brush regimes, Biochim. Biophys. Acta 1564 (2002) 237–242.
[49] D. Paolino, R. Muzzalupo, A. Ricciardi, C. Celia, N. Picci, M. Fresta, In vitro and in vivo evaluation of Bola-surfactant containing niosomes for transdermal delivery, Biomed. Microdevices 9 (2007) 421–433.
[50] J. Wolfram, K. Suri, Y. Yang, J. Shen, C. Celia, M. Fresta, Y. Zhao, H. Shen, M. Ferrari, Shrinkage of pegylated and non-pegylated liposomes in serum, Colloids Surf. B: Biointerfaces 114 (2014) 294–300.